Si(100)-(2×1)boron reconstruction: Self-limiting monolayer doping

R. L. Headrick, B. E. Weir, A. F. J. Levi, D. J. Eaglesham, and L. C. Feldman
AT&T Bell Laboratories, Murray Hill, New Jersey 07974

(Received 16 July 1990; accepted for publication 25 September 1990)

A (2×1) surface reconstruction distinct from the clean Si(100)-(2×1) surface is formed by depositing boron onto silicon in ultrahigh vacuum. Overgrowth of epitaxial silicon at low temperature preserves a (2×1) superstructure of substitutional boron. Hall-effect measurements at 4.2 K show complete electrical activity for boron coverages of 1/2 monolayer, but additional boron above 1/2 monolayer is not electrically active.

Two-dimensional, metastable, ordered structures have recently been preserved by preparing Si(111) surface reconstructions under epitaxially grown overlayers of silicon.[1–4] These new structures are possible because epitaxial films of silicon[5,6] and other materials can be grown at temperatures below that for thermal disordering of the original structure. The discovery that surface superlattice structures can be buried in crystalline semiconductors suggests possibilities for monolayer doping profiles and ordered doping/alloy structures with new electronic properties.

In this letter, we report a boron-induced (2×1) surface reconstruction at 1/2 monolayer boron coverage on ⟨100⟩ oriented silicon, where 1 monolayer is defined as 6.8×10^{14} cm^{-2}. To our knowledge this reconstruction has not been reported previously. We find that this reconstruction can be preserved within high quality crystalline silicon by low-temperature epitaxial overgrowth at ≈300 °C, in contrast to the clean Si(100)-(2×1) reconstruction which is removed even by room-temperature deposition. For boron coverages at and below the completion of the (2×1) surface phase and silicon overlayer growth temperatures of 300 °C, 100% of the boron is electrically active, while at higher coverages the excess boron, which occupies a different surface site, does not become electrically active. The doping is thus "self-limiting" since boron atoms cover the surface and prevent other boron from becoming electrically active.

Samples were prepared in a molecular beam epitaxy chamber equipped with an electron gun evaporator to deposit silicon, a quartz-crystal thickness monitor, and a Knudsen cell to deposit boron from HBO_2. Samples of (300 Ω cm) *n*-type ⟨100⟩ oriented Si were prepared by chemical growth of a thin protective oxide layer, and then transferred into the vacuum chamber. Once in the vacuum chamber, the oxide was desorbed from the sample and boron was deposited onto the surface held at 500 °C up to a coverage of between 0 and 1 monolayer. A 30 s anneal at 700 °C desorbed any remaining oxygen from the surface. After cooling to room temperature, low-energy electron diffraction (LEED) and Auger electron spectroscopy measurements were performed. Finally, the surface was capped with 100 Å of silicon at either room temperature, or ≈300 °C. All other measurements, including grazing incidence x-ray diffraction, ion scattering/channeling, transmission electron microscopy, and low-temperature ($T=4.2$ K) Hall-effect measurements were done after removing the capped samples from the vacuum system.

Figure 1(a) shows the initial clean surface Si(100)-(2×1) LEED pattern at 61 eV. The pattern shows a bright, two-domain (2×1) reconstruction where the two domains are rotated by 90° with respect to one another. This well-known diffraction pattern occurs on (100) silicon surfaces when monolayer-high steps are present on the surface; then there are two orthogonal Si-Si dimer orientations giving rise to the two orthogonal (2×1) domains. Figure 1(b) shows the 61 eV LEED pattern from a Si(100) surface with 1/2 monolayer boron coverage. The pattern symmetry is similar to that in Fig. 1(a) in that a two domain (2×1) reconstruction is again present. However, differences in the ratio of intensities as compared to the pattern in Fig. 1(a) are apparent. In particular, the

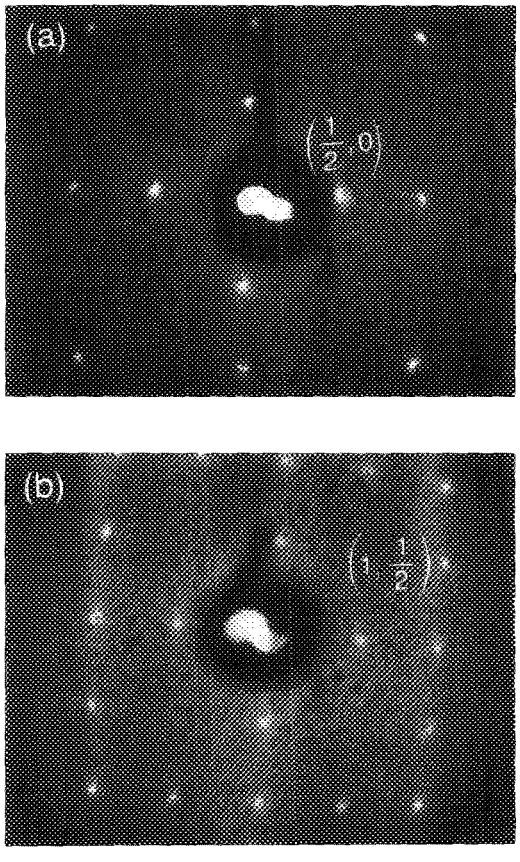

FIG. 1. Low-energy electron diffraction patterns at 61 eV. (a) Clean Si(100)-(2×1), (b) Si(100)-(2×1) boron.

 0003-6951/90/522779-03$02.00

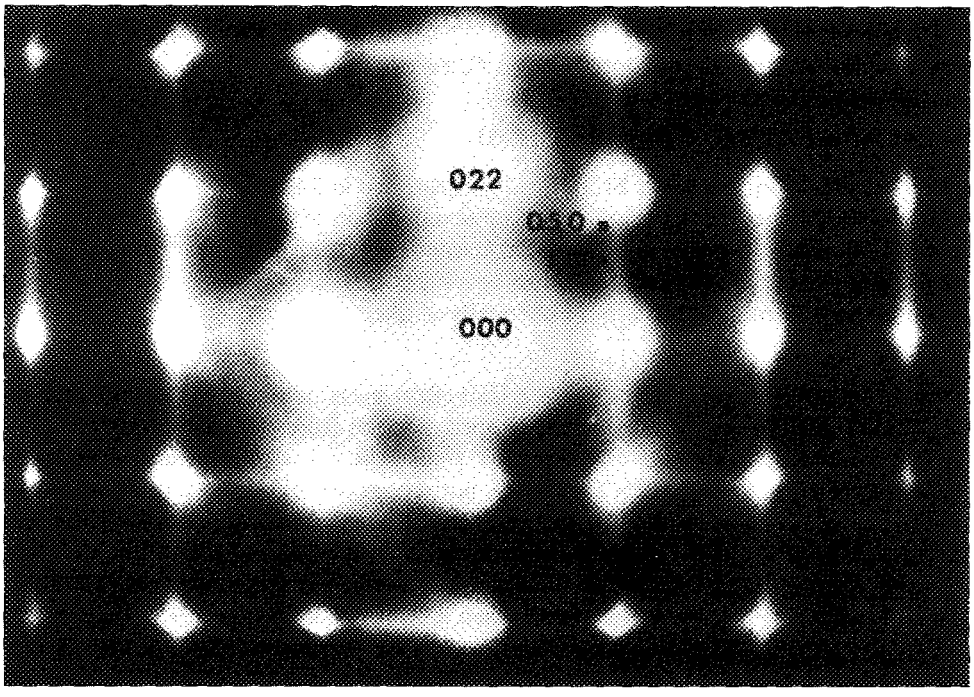

FIG. 2. Transmission electron diffraction pattern of Si(100)-(2×1)boron with an epitaxial silicon cap grown at room temperature.

(1,1/2) spot is the most intense half-order spot in the diffraction pattern from the boron-covered surface [Fig. 1(b)], while the (1/2,0) spot is the most intense half-order in the diffraction pattern from the clean surface [Fig. 1(a)]. Although the LEED data is only at a single voltage, it shows that the LEED intensity versus voltage curves for the two structures would be different and that the two surface structures are different. This striking difference was reproduced many times with three different LEED apparatuses. Also, the original clean surface pattern returns after silicon epitaxial overgrowth which buries the boron layer. Therefore, adsorption of boron onto clean Si(100) can induce a new surface reconstruction with the same periodicity as the clean surface reconstruction.

Boron coverages above 1/2 monolayer result in a higher background in LEED, and a sharply decreased grazing incidence x-ray half-order diffraction intensity. This shows that boron in excess of 1/2 monolayer does not occupy a well-ordered site. Thus we believe that a Si(100)-(2×1)boron surface phase, possibly with some disorder, is completed at 1/2 monolayer coverage corresponding to one boron atom per unit cell of the reconstruction.

We now consider the behavior and preservation of the ordered boron structure under different conditions of silicon overgrowth. Figure 2 shows the transmission electron diffraction pattern for the Si(100)-(2×1) boron ordered interface structure capped with silicon at room temperature. Sharp diffraction spots arising from a two-dimensional layer with double the surface period are present and both (2×1) domains are observed. It is known,[7] and we also confirm, that the (2×1) reconstruction of the *clean* silicon surface is not preserved during room-temperature molecular beam overgrowth of silicon. This behavior is readily understood in terms of the silicon dimer surface structure: during room temperature overgrowth, the dimer bond is broken, the double periodicity is removed, and a few layers of epitaxial growth take place under some growth conditions. The existence and thickness of the epitaxial part of the deposited silicon depends sensitively on the temperature of the sample, the growth rate, and the surface preparation.[5]

Figure 3 shows grazing incidence x-ray diffraction azimuthal scans through (3/2,0) surface reflections for two ordered interfaces. The open circles are for a 100 Å cap grown at room temperature, and the filled circles are for a 100 Å cap grown at 300 °C. The boron coverage is 1/2 monolayer in both cases. Comparison of the data in Fig. 3 demonstrates that the reconstruction capped at 300 °C gives a factor of two smaller integrated intensity in the diffraction signal than the reconstruction capped at room temperature. Boron segregation studies using Auger electron spectroscopy for films grown at 300 °C reveal a broadening of the ideal monolayer distribution by ≈5 Å. This is consistent with the observation that ≈50% of the boron remains in the ordered layer.

Cross-sectional transmission electron microscopy and ion channeling studies show that the 100-Å-thick films

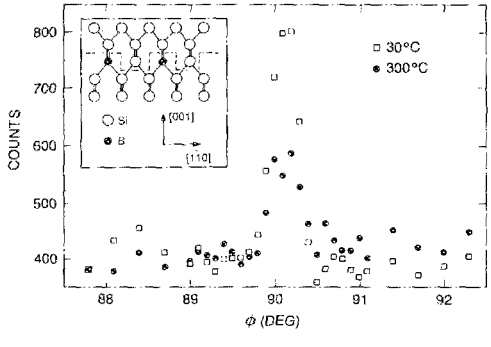

FIG. 3. Comparison of grazing incidence x-ray diffraction azimuthal scans through the (3/2,0) diffraction spot for Si(100)-(2×1)boron buried structures capped by growth at room temperature, and at ≈300 °C. The boron coverage was 1/2 monolayer in both cases and the silicon growth rate was 0.1 Å/s. The inset shows a model of the (2×1) structure.

Boron coverages, carrier densities, and mobilities for silicon films grown and annealed at various temperatures.

Film thickness (Å)	T_{growth} (°C)	T_{anneal} (°C)	Anneal time (min.)	Boron coverage (ML)	Carrier density (ML)	Mobility ($cm^2 V^{-1} s^{-1}$)
100	30	···	···	0.50	0.24	1
100	30	···	···	0.50	0.18	3
100	30	450	1	0.11	0.07	14
100	30	450	1	0.31	0.18	21
100	30	450	1	0.51	0.32	16
100	30	450	1	0.83	0.33	18
100	300	···	···	0.44	0.45	21
350	400	···	···	0.24	0.28	31
350	400	···	···	0.88	0.66	39
350	450	···	···	0.24	0.28	35
350	450	···	···	0.88	0.66	41

grown at 300 °C are high quality crystalline silicon indistinguishable from bulk silicon, while room-temperature growth results in an amorphous layer. Channeling measurements in ⟨100⟩ normal incidence and ⟨111⟩ off-normal incidence using the $^{11}B(p,\alpha)\,^{8}Be$ nuclear reaction to detect boron, show a reduced yield compared to random incidence after silicon overgrowth at 300 °C, indicating that boron occupies a substitutional site buried within crystalline material. After room-temperature overgrowth, channeling does not reduce the yield from the boron since the film is amorphous. A model of the buried structure is shown in the inset of Fig. 3; the dashed line separates the original boron-covered surface from the silicon overgrowth. In this diagram, we assume that boron occupies sites on top of the surface, although we cannot rule out the possibility that some (or all) of the boron occupies subsurface sites. Boron is known to occupy a subsurface site in the boron-stabilized $(\sqrt{3}\times\sqrt{3})$ surface of ⟨111⟩ oriented silicon.[3,8]

We now discuss the electrical activity of boron-doped silicon structures prepared via the (2×1) reconstruction. There was no carrier freeze-out and no significant magnetoresistance for any of the samples measured. The optimum conditions for producing electrically active ordered doping layers in epitaxial silicon are a boron coverage of 1/2 monolayer and a silicon growth temperature of 300 °C as shown in Table I. Under these conditions 100% electrical activity and a mobility of 21 $cm^2 V^{-1} s^{-1}$ are obtained. This mobility is comparable to that obtained for very high boron concentrations in bulk silicon.[9]

Figure 4 shows carrier density as a function of boron coverage. These samples were capped with 100 Å of silicon at room temperature and annealed briefly at 450 °C. The room-temperature deposit always produces doping layers with less than 100% electrical activation; however, the data contain interesting information about the effect of the saturation coverage of boron in the (2×1) reconstruction on the electrical activity. The *p*-type carrier density is found to increase linearly with boron coverage up to a coverage of 1/2 monolayer with ≈65% electrically active boron, but higher boron coverages show no further increase in the carrier density above that reached at 1/2 monolayer. There are a limited number of ordered sites

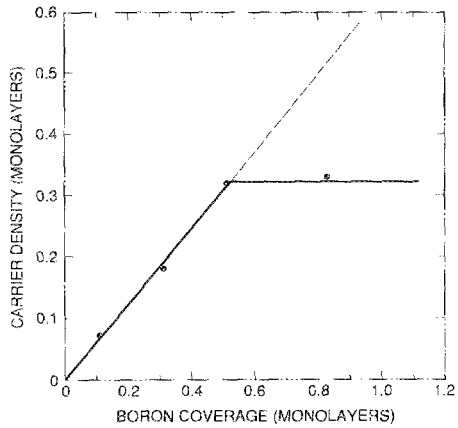

FIG. 4. Carrier density and carrier mobility at 4.2 K as a function of boron coverage for boron monolayer doping layers. Ordered Si(100)-(2×1) boron surfaces were capped at room temperature and annealed to 450 °C for 1 min.

available for boron in the stable (2×1) reconstruction, so that above the saturation coverage of the reconstruction additional boron atoms cannot occupy epitaxial sites. Instead, they may form dimers or clusters that are not broken up during epitaxial growth, or they may become interstitial atoms that are not electrically active. This self-limiting effect is reduced during growth at higher temperatures; however, a growth temperature of 450 °C at 0.88 monolayer coverage still results in less than 100% electrical activation.

In conclusion, we have observed a boron-induced (2×1) surface reconstruction. This reconstruction is maintained following low-temperature epitaxial overgrowth, and the electrical activity of boron in the buried structure is correlated with ordered and disordered surface sites of boron. Complete (100%) electrical activity is obtained for ordered boron monolayer doping at 1/2 monolayer coverage and a growth temperature of 300 °C. Monolayer doping in high quality crystalline material suggests possibilities for materials with new electronic properties and for improved semiconductor devices.

We thank C. T. Chen, K. Evans-Lutterodt, Y. Ma, I. K. Robinson, and F. Sette for valuable contributions.

[1] K. Akimoto, J. Mizuki, I. Hirosawa, T. Tatsumi, H. Hirayama, N. Aizaki, and J. Matsui, *Extended Abstracts on the 19th Conference on Solid State Devices and Materials* (Business Center for Academic Societies, Tokyo, 1987), p. 463.
[2] R. L. Headrick, L. C. Feldman, and I. K. Robinson, Appl. Phys. Lett. **55**, 442 (1989).
[3] R. L. Headrick, I. K. Robinson, E. Vlieg, and L. C. Feldman, Phys. Rev. Lett. **63**, 1253 (1989).
[4] R. L. Headrick, B. E. Weir, J. Bevk, B. S. Freer, D. J. Eaglesham, and L. C. Feldman, Phys. Rev. Lett. **65**, 1128 (1990).
[5] D. J. Eaglesham, H.-J. Gossmann, and M. Cerullo, Phys. Rev. Lett. **65**, 1227 (1990).
[6] H. Jorke, H.-J. Herzog, and H. Kibbel, Phys. Rev. B **40**, 2005 (1989).
[7] J. M. Gibson, H.-J. Gossmann, J. C. Bean, R. T. Tung, and L. C. Feldman, Phys. Rev. Lett. **56**, 355 (1986); H.-J. Gossmann, L. C. Feldman, and W. M. Gibson, *ibid.* **53**, 294 (1984); Surf. Sci. **155**, 413 (1985); H.-J. Gossmann and L. C. Feldman, Phys. Rev. B **32**, 6 (1985).
[8] P. Bedrossian, R. D. Meade, K. Mortensen, D. M. Chen, and J. A. Golovchenko, Phys. Rev. Lett. **63**, 1257 (1989); I.-W. Lyo, E. Kaxiras, and Ph. Avouris, Phys. Rev. Lett. **63**, 1261 (1989).
[9] G. Masetti, M. Severi, and S. Solmi, IEEE Trans. Electron. Dev. **30**, 764 (1983).